FEBS Letters 586 (2012) 1147–1153

journal homepage: www.FEBSLetters.org

The crystal structure of the MPN domain from the COP9 signalosome subunit CSN6

Heng Zhang [a,b], Zeng-Qiang Gao [b], Wen-Jia Wang [b], Guang-Feng Liu [b], Eleonora V. Shtykova [c], Jian-Hua Xu [b], Lan-Fen Li [a], Xiao-Dong Su [a,*], Yu-Hui Dong [b,*]

[a] State Key Laboratory of Protein and Plant Gene Research, and Biodynamic Optical Imaging Center (BIOPIC), School of Life Sciences, Peking University, No. 5 Yiheyuan Road, Beijing 100871, China
[b] Beijing Synchrotron Radiation Facility, Institute of High Energy Physics, Chinese Academy of Sciences, Beijing 100049, China
[c] Institute of Crystallography, Russian Academy of Sciences, 59 Leninsky Pr., 117333 Moscow, Russia

ARTICLE INFO

Article history:
Received 17 February 2012
Revised 8 March 2012
Accepted 9 March 2012
Available online 23 March 2012

Edited by Christian Griesinger

Keywords:
MPN domain
JAMM motif
COP9 signalosome
CSN6
Crystal structure

ABSTRACT

The COP9 signalosome (CSN) is a multiprotein complex containing eight subunits and is highly conserved from fungi to human. CSN is proposed to widely participate in many physiological processes, including protein degradation, DNA damage response and signal transduction. Among those subunits, only CSN5 and CSN6 belong to JAMM family. CSN5 possesses isopeptidase activity, but CSN6 lacks this ability. Here we report the 2.5 Å crystal structure of MPN domain from *Drosophila melanogaster* CSN6. Structural comparison with other MPN domains, along with bioinformation analysis, suggests that MPN domain from CSN6 may serve as a scaffold instead of a metalloprotease.

Structured summary of protein interactions:
CSN6 and **CSN6** bind by x-ray crystallography (View interaction)
CSN6 and **CSN6** bind by x ray scattering (View interaction)

1. Introduction

The COP9 signalosome, generally named CSN, is composed of eight subunits (CSN1–CSN8) and exists in all eukaryotes [1]. It seems that the complex is somewhat unstable and can be subdivided into a series of subcomplexes relevant to different functions [2]. Among those components, only CSN5 and CSN6 share an MPN (Mpr1p and PAD1p N-terminal) domain. The other subunits defines a common motif named PCI (proteasome, COP9 signalosome, and initiation factor) [4,5]. The two distinct domains are also found in 26S proteasome and eukaryotic translation initiation factor 3. It is believed that these three complexes interact with each other [6].

COP9 signalosome was first described as a repressor of photomorphogenesis in *Arabidopsis* by Deng and his collaborators [7]. In recent years, CSN has been found to take part in a variety of physiological processes, such as cell cycle, subcellular localization and transcriptional regulation [8]. So far, the property which has been studied most is ubiquitin-associated degradation in protein quality control. This function is fulfilled by removal of Nedd8/Rub1 (an ubiquitin-like molecule) from the cullin subunit of E3 ligases. The deneddylation process is mediated by CSN5. More precisely, the JAMM (Jab1/MPN/Mov34) motif located in the MPN domain cleaves Nedd8 as a metalloprotease [9,10]. Nevertheless, CSN5 alone has no metalloprotease activity unless it is associated with other subunits. A conserved sequence termed JAMM motif was first defined in *Archaeoglobolus fulgidus* Af2198 [13,14]. JAMM motif is responsible for zinc coordination and cleavage of Nedd8. Much evidence reveals that there are two types of MPN domains: one, like CSN5 with JAMM motif, has the metalloprotease activity while another, the same as CSN6 without JAMM motif, has no related isopeptidase activity. The role of MPN domain without JAMM motif is still unclear, but recent studies have shown that such MPN domains can be employed to mediate protein–protein interactions [16,17]. CSN6 makes a contribution to the binding of CSN and E3 ligases [9,10], and directly binds to MDM2, which is an ubiquitin ligases correlated with p53 pathway [11]. MPN domain maybe serves as a scaffold in those processes.

We have tried to get the full length CSN6 protein. Unfortunately, the full length protein is mostly insoluble by expressing in *E. coli*. Yet in the soluble portions appear self-aggregation and precipitation, even though treated with 2 M urea, 2 M NaCl or 5% PEG8000. This finding is consistent with previous observations that soluble full-length CSN6 could be obtained by coexpression of other subunits [2]. In order to understand the role of MPN domain in CSN, we determined the crystal structure of CSN6 MPN domain (residues 51–187) from *Drosophila melanogaster* at 2.5 Å.

Several MPN-containing proteins that derived from various species were obtained and their structures were solved by X-ray crystallography [13–19]. Structural comparison of these proteins and

* Corresponding authors.
E-mail addresses: xdsu@pku.edu.cn (X.-D. Su), dongyh@ihep.ac.cn (Y.-H. Dong).

0014-5793/$36.00 © 2012 Federation of European Biochemical Societies. Published by Elsevier B.V. All rights reserved.
http://dx.doi.org/10.1016/j.febslet.2012.03.029

bioinformation analysis of CSN6 MPN domain offer clues to investigate the evolution of JAMM family members and to broaden our understanding of CSN6 function.

2. Materials and methods

The expression, purification, crystallization of the CSN6 MPN domain, X-ray data collection, structure determination and refinement, SAXS data collection and analysis are described in Supplementary material.

The final refinement statistics are shown in Table 1. All molecular figures were prepared using PyMOL [21]. The multiple sequence alignment figure was generated using ClustalW [22] and ESPript [23]. The degree of surface conservation was estimated using program ConSurf [24].

3. Results and discussion

3.1. Overall structure and oligomeric state of CSN6$^{51-187}$

The crystal structure of *D. melanogaster* CSN6$^{51-187}$ has been determined to 2.5 Å. The crystal belongs to the space group $P4_32_12$ and contains two molecules, A&B, per asymmetric unit. Loop2 (Arg72-Glu77), loop8 (Asn143-Ile149) in both molecules could not be modelled. Additionally residues 185–187 in molecule A, residues 106–111 and 177–184 in molecule B are disordered and also could not be modelled. Since molecule A had less missing fragments it was chosen for discussion in this paper, unless otherwise noted.

The structure of molecule A is mainly composed of seven β-strands and four α-helices (Fig. 1A, 1B). In the center of the structure, five β-strands (β1–β3, β6 and β7) form a β-antiparallel sheet flanked by three α-helices (α1, α2 and α4) and a β-hairpin (β4–β5). Helix α3 folds onto the entrance of the protein core. The structure of CSN6$^{51-187}$ is similar to other members of MPN family, whereas there are two insertions compared with *A. fulgidus* Af2198 [13,14]. One insertion, α4 helix, occurs at the C-terminal and the other one is located in the side of the protein, including a β-hairpin and the following α2 helix.

CSN6$^{51-187}$ migrates as a dimer through a Superdex 200 gel filtration column (data not shown), which is consistent with the crystal structure (Fig. 1A). There are two stable forms of the dimer based on the *PISA* result and interface analysis [3]. The asymmetric unit of our crystal structure comprises the AB type of the dimer with a non-crystallographic twofold axis (Fig. 1A). The other form of the dimer (BB́) is created by packing (Fig. 1C). The interface areas in AB and BB́ form are 965.4 and 694.6 Å^2, respectively, suggesting that the dimer observed in the asymmetric unit (AB) is a biological form.

Additional and independent evidence of the dimerization of the CSN6$^{51-187}$ could be provided by an analysis of small-angle X-ray scattering data. Fig. 2A demonstrates the experimental SAXS curve, and theoretical scattering curves calculated by the program CRYSOL from AB (curve 2) and BB́ (curve 3) dimers. The scattering curve calculated from dimer AB fits experimental data much better than from BB́ one. Thus, we can conclude that the AB conformation represents the actual status of the CSN6$^{51-187}$ in solution. However, we should aware that a structure in crystal and in solution can be different. Therefore, an attempt was made to restore a low resolution structure of the protein in solution using ab initio procedure. Fig. 2B shows the results of shape restoration by the program DAMMIN (curve 3, model b) [26], and by the program GASBOR (curve 4, model c) [25]. Corresponding distance distribution function and back transformed from *p(r)* function curve extrapolated to zero scattering angle are also presented in Fig. 2B. All model curves demonstrate practically ideal fits to the experimental data with the discrepancy of about 0.8. Superposition of the available crystal structure of the AB dimer (Fig. 2B, structure a) and of the obtained low resolution models shows their similarity. Thus, undertaken analysis of SAXS data clearly points to the formation of the AB dimeric conformation of the CSN6$^{51-187}$ in solution.

3.2. Dimer interface

Dimerization of CSN6$^{51-187}$ (AB type) occurs through the interaction of β1 and β7 strands in both molecules. The interface consists mainly of hydrophobic residues, which form a hydrophobic core. The hydrogen bonds are formed in both molecules between main chain atoms of Val52 and Leu167, Ile54 and Leu165, Leu65 and Ile 163, as well as the hydroxyl group of Ser51 in molecule B and the carbonyl of Asn168 in molecule A. In addition, Glu160 in molecule B protrudes away from the interface surface and makes two salt bridges to His57 of molecule A (Fig. 1D).

For DmCSN5, *Tango* server [20] predicts some regions involved in β-aggregation (Supplementary Fig. 1). Two segments corresponding to CSN6$^{51-187}$, β1 and β7, are highly aggregation-prone, especially residues 162–167. Moreover, those residues involved in interface interactions in CSN6$^{51-187}$ can be found in the two regions. We can conclude that CSN6$^{51-187}$ dimeric interactions may provide the basis for CSN5 homodimer or CSN5-CSN6 heterodimer [28–30]. It is also possible that the association of CSN-based supercomplexs is mediated via MPN domains [15,31].

Dimerization has also been reported in the Rpn8 structure [15]. Rpn8, which has an MPN domain, is a subunit of 26S proteasome. However the biological dimer in Rpn8 is not the asymmetric unit which is composed of two molecules. Authors defined another dimer resulted from the crystal packing by *PISA* and interface analysis. Moreover, the interactions of the interface in Rpn8 are distinct from those observed in the present structure. The dimer

Table 1
Data collection and structure refinement statistics.

Data collection	
Data collection	
Wavelength (Å)	0.9794
Space group	$P4_32_12$
Unit-cell parameters	a = b = 109.062, c = 46.437
Resolution (Å)	2.50 (2.54–2.50)[a]
Number of unique reflections	10201(494)
Completeness (%)	99.8 (100)
Redundancy	25.4(27.8)
Mean I/σ (I)	84.2(11.0)
Molecules in asymmetric unit	2
R_{merge} (%)	9.9 (51.1)
Structure refinement	
Resolution range (Å)	33.63–2.50
R_{work}/R_{free} (%)	23.2/26.1
Average B factor (Å^2)	
Main chain (chain A/B)	61.5/67.5
Side chain (chain A/B)	64.4/72.3
Waters	52.5
Ramachandran plot (%)	
Most favoured	97.2
Allowed	2.8
Disallowed	0.0
r.m.s. deviations	
Bond lengths (Å)	0.009
Bond angles (°)	1.219

[a] The values in the parentheses refer to those of highest resolution shell.

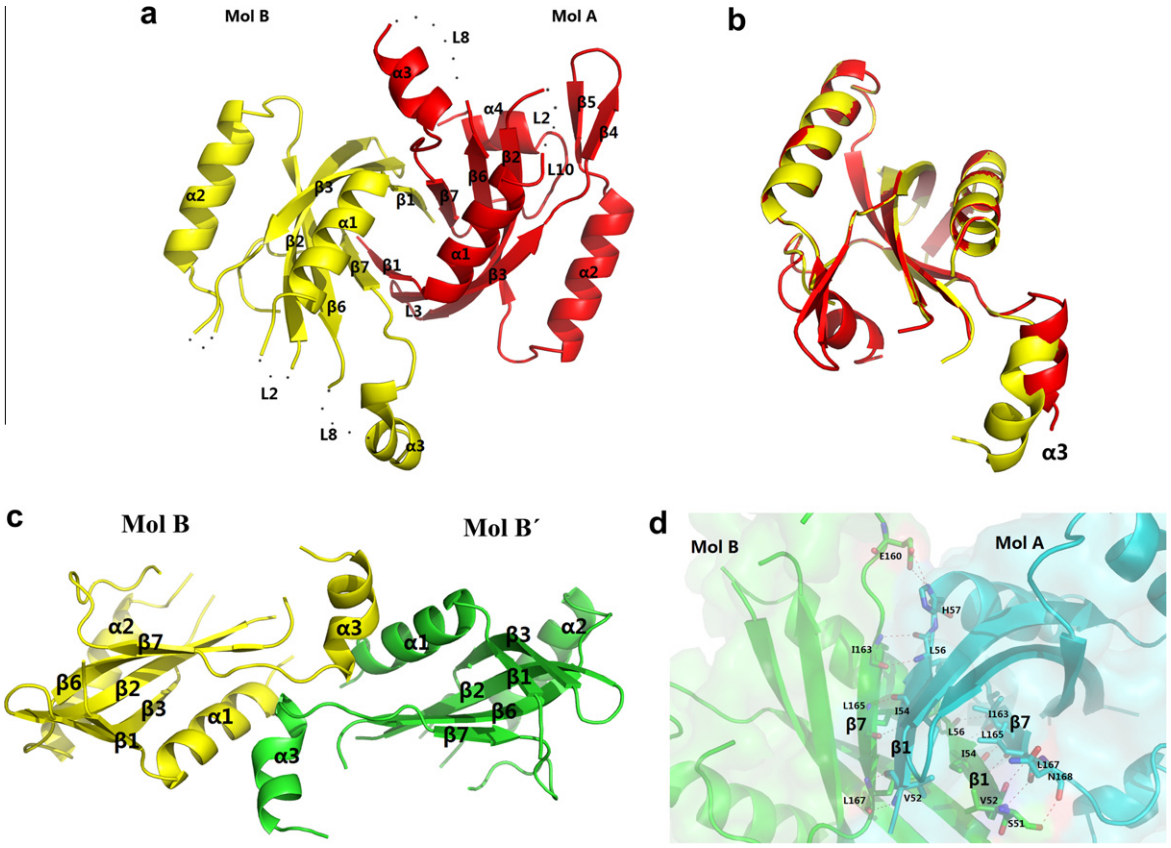

Fig. 1. Overall structure of MPN domain from CSN6. (a) The molecule A is in red and molecule B is in yellow. The disorder regions are shown as gray dotted lines. (b) Superposition of molecule A and molecule B. Molecule A is in good agreement with molecule B except the helix α3. Colour schemes are the same as in (a). (c) Ribbon model of BB́dimer. This type dimer is created by crystal packing with symmetry-related molecules (symmetry mate $x, y, -z+1$). (d) Interface between molecule A and molecule B. Residues are shown in sticks representation. The hydrogen and salt bonds are indicated by red dashed lines.

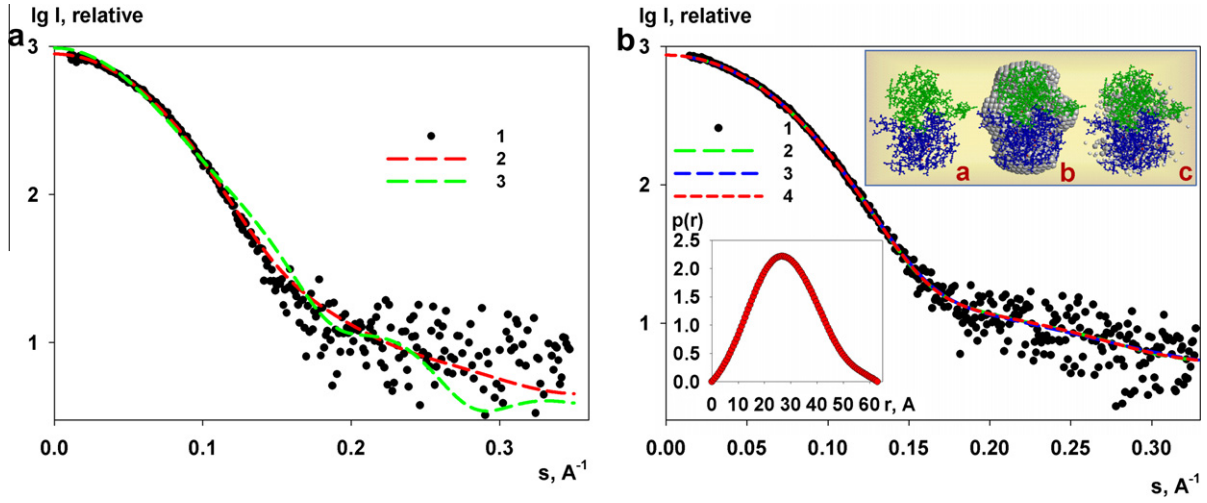

Fig. 2. Experimental scattering curve from the $CSN6^{51-187}$ in solution and modelling. (a): 1 – experimental SAXS curve; 2 – theoretical scattering from the high resolution structure of AB dimer calculated by the program CRYSOL; 3 – theoretical scattering from the high resolution structure of BB́ dimer calculated by the program CRYSOL. (b): 1 – experimental SAXS curve; 2 – scattering patterns computed from the DAMMIN model; 3 – scattering patterns computed from the GASBOR model; 4 – smooth curve back transformed from *p(r)* and extrapolated to zero scattering angle for the $CSN6^{51-187}$. Inserts: right above – models: a – crystal structure of the AB dimer; b – superposition of DAMMIN model and the crystallographic structure of the AB dimer; c – superposition of GASBOR model and the crystallographic structure of the AB dimer; left below – the distance distribution functions *p(r)* computed by the program GNOM for $CSN6^{51-187}$ in solution.

interface of Rpn8 contains hydrophobic interactions and hydrogen bonds, and involves three helices (α1, α2 and α4) and their connecting loops. These differences may be responsible for different biological functions.

3.3. Conserved Amino Acids and molecular surface properties

A multiple sequence alignment of *D. melanogaster* MPN domain with its homologues shows a high degree of identity (Fig. 3A).

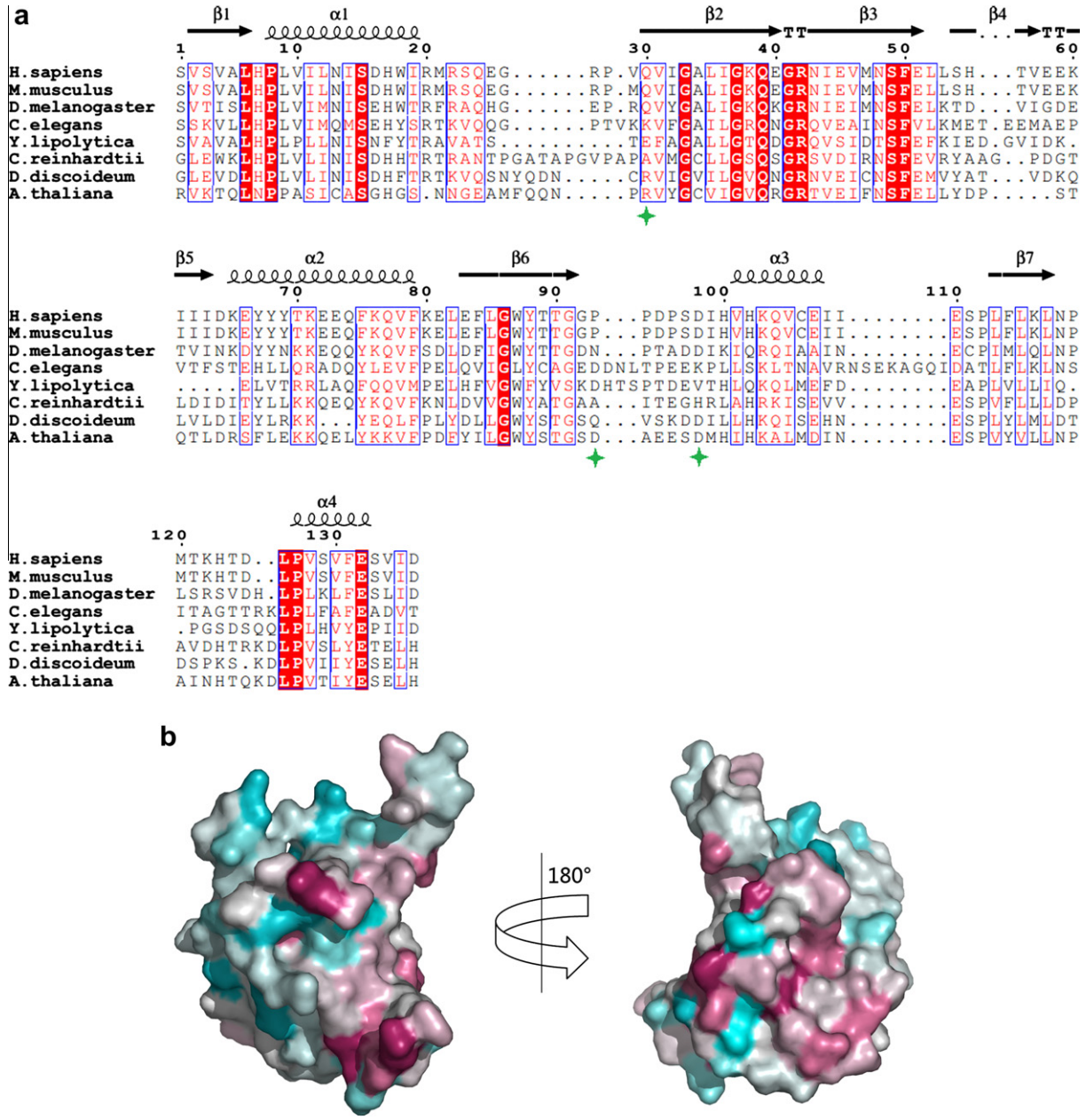

Fig. 3. (a) Structure based sequence alignment of CSN6 MPN domains. The sequences of MPN domains are from *H. sapiens* (UniProt ID: Q7L5N1), *Mus musculus* (UniProt ID:Q3UIT2), *D. melanogaster* (UniProt ID:Q9VCY3), *Caenorhabditis elegans* (UniProt ID:Q95PZ0), *Yarrowia lipolytica* (UniProt ID: Q6C7M5), *Chlamydomonas reinhardtii* (UniProt ID: Q2MJW1), *Dictyostelium discoideum* (UniProt ID: Q54C92) and *Arabidopsis thaliana* (UniProt ID:Q8W206). Strictly conserved residues are shown with a red background and conserved residues are coloured red. Residues similar to the JAMM motif are indicated by green stars. (b) Conserved residues are mapped onto the CSN6$^{51-187}$ surface. Highly conserved residues are shown in maroon, and most variable residues are shown in cyan.

When the results are mapped onto our structure, the majority of the conserved residues are found to be solvent-exposed (Fig. 3B). Despite the invariant residues are widely distributed throughout the protein, most of them are concentrated in the secondary structural elements. Meanwhile, there are several invariant residues buried in the interior of the protein, including eight non-polar amino acids (Leu56, Val60, Val80, Gly83, Leu85, Gly136, Leu165 and Leu177) forming a hydrophobic patch. The residues that make up the dimer interface are also highly conserved, which means that they may play an important role in CSN6 functions and association.

The electrostatic surface potential is employed to study the features of the present structure. CSN6$^{51-187}$ is strongly electronegative in agreement with its theoretical isoelectric point of 5.7, with fragmented regions of positive potential, such as α3, loop3 and part of α2 (Fig. 4A). The β4-β5 hairpin together with two helices (α3 and α4) forms a groove facing the solvent. This groove is implied to be a site of substrate binding or protein interaction. Apart from the charged surface, the residues involved in the groove are well conserved (Fig. 3A). Therefore, further investigation of the groove role in CSN6 and signalosome is essential.

3.4. Pseudo Motif

CSN5 and Rpn11 have isoprotease activity with a canonical metalloenzyme motif [16]. The metal-binding motif, known as JAMM and referred to as EXnHXHX$_7$SX$_2$D, was first identified in *A. fulgidus* Af2198 [13,14]. In contrast, there is no such motif in CSN6. However, several residues that similar to the JAMM motif

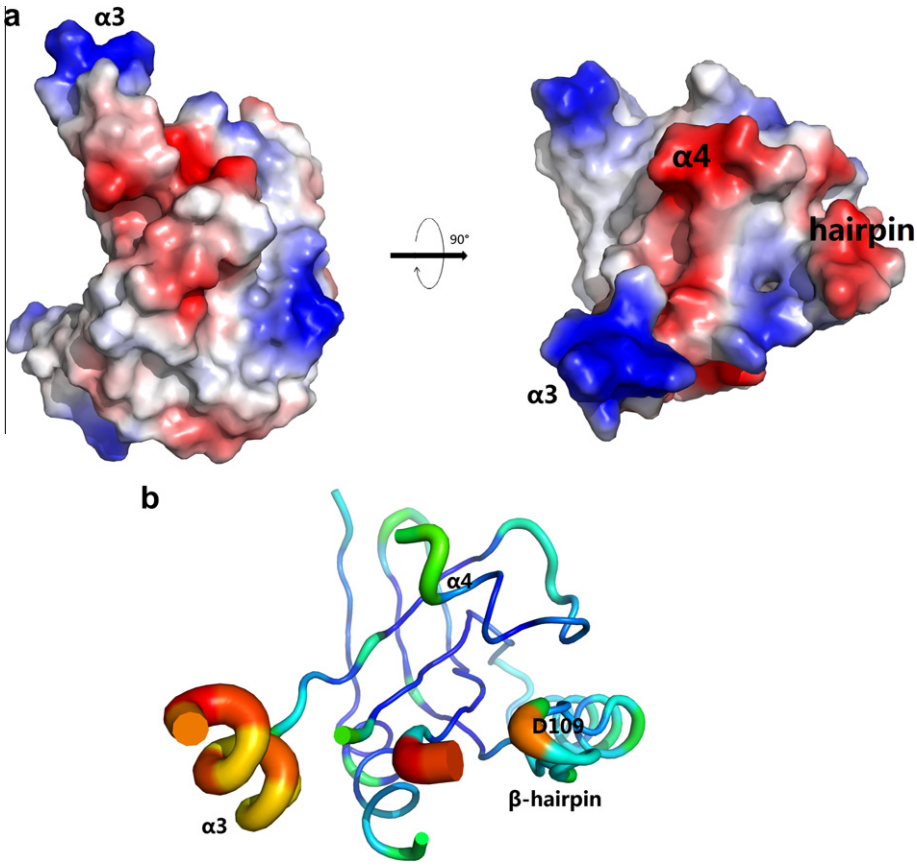

Fig. 4. (a) Electrostatic surface potential of CSN6$^{51-187}$ structure. Blue and red are positively and negatively charged, respectively. Grey represents neutral potential. The positions of some regions mentioned in the article are labelled. (b) B-factor putty representation of CSN6$^{51-187}$. The overall structure is well-ordered except helix α3 and the following loop. Note that the residue Asp109 appears flexible with high B-factor.

in CSN6$^{51-187}$ are found in the equivalent position and located in a loop (loop8) connecting a β strand (β6) and α helix (α3) (Fig. 1A). Neither metal atom nor water molecule that occupies a position equivalent to the zinc ion was found. Moreover, there is no significant anomalous X-ray scattering signal in native CSN6$^{51-187}$ crystals. MPN domains from Rpn8 and Prp8 exhibit a partially lacked and non-conserved JAMM motif, but they also have no ability to bind Zn^{2+}[15–17]. The above analysis indicates that JAMM motif integrity is highly important to bind zinc ion. Interestingly, the pseudo JAMM motif is not conserved in *D. melanogaster* CSN6 and its orthologs (Fig. 3A). Previous studies have shown that JAMM motif is not essential for function of inactive MPN domains according to the biochemical and mutational analysis [27]. Thus, we can conclude that this pseudo motif in CSN6 has no physiological functions along with the loss of the isopeptidase activity.

3.5. Comparisons with MPN homologues

The model of CSN6$^{51-187}$ was submitted to the *DALI* server [12] to identify a range of structural related proteins. According to the search results, a number of structural homologues were found, including *Homo sapiens* Rpn8 (26S proteasome regulatory subunit N8; PDB entry 2O96), *Homo sapiens* AMSH-LP (STAM binding protein-like 1; PDB entry 2ZNR), *A. fulgidus* Af2198 (hypothetical protein; PDB entry 1OI0), *Saccharomyces cerevisiae* Prp8 (pre-mRNA splicing factor; PDB entry 2OG4). All of those proteins display a canonical MPN domain core [13–19]. Despite the low sequence homology (17%), CSN6 MPN domain is similar to other MPN members in architecture, adopting a three-layer sandwich fold.

In addition to structural similarity in all of MPN domains, the CSN6$^{51-187}$ protein exhibits several unique characteristics that may be important to CSN6 function (Fig. 5A).

The most prominent difference is the protruding helix α3. In CSN6$^{51-187}$, helix α3 introduces ~90° bend along the corresponding helix in other proteins. Superimpositions of chain A and chain B result in r.m.s.d value of 0.352 Å (121 Cα atoms) (Fig. 1B). The only notable difference is the helix α3. It is tempting to explain the matter by a considerable flexibility of this segment. Evidently, B-factor of α3 helix is significantly higher and tends to correlate with structural flexibility. It is worth noting that the pseudo JAMM motif resides in this region. In addition to the partial motif, loop8 is also incompletely traced, probably due to the conformational flexibility (Figs. 1A, 4B). Furthermore, this helix interacts with neighbouring molecules in the crystal lattice via a combination of salt bonds and hydrogen bonds (Fig. 5B). Together, it is possible to deduce that this segment participates in the protein–protein interaction rather than in binding of the substrate as a pocket. Helix α3 expands away from the MPN core and may be relevant to an unknown functional area.

Intriguingly, helix α4, observed in the present structure, corresponds to helix α3 in other JAMM family structures [15–19]. It seems that the place where helix α3 should reside in is taken by shorter helix α4 and the following loop10. In AMSH-LP, there are several residues from helix α3 involved in the distal ubiquitin binding [18]. These equivalent residues are not observed in α3 helix of CSN6$^{51-187}$, but appear in α4 helix and loop10. Among these residues, Ser173 and Asp175 are absolutely conserved, and Thr363 in AMSH-LP is converted to Ser184 in CSN6$^{51-187}$. These observa-

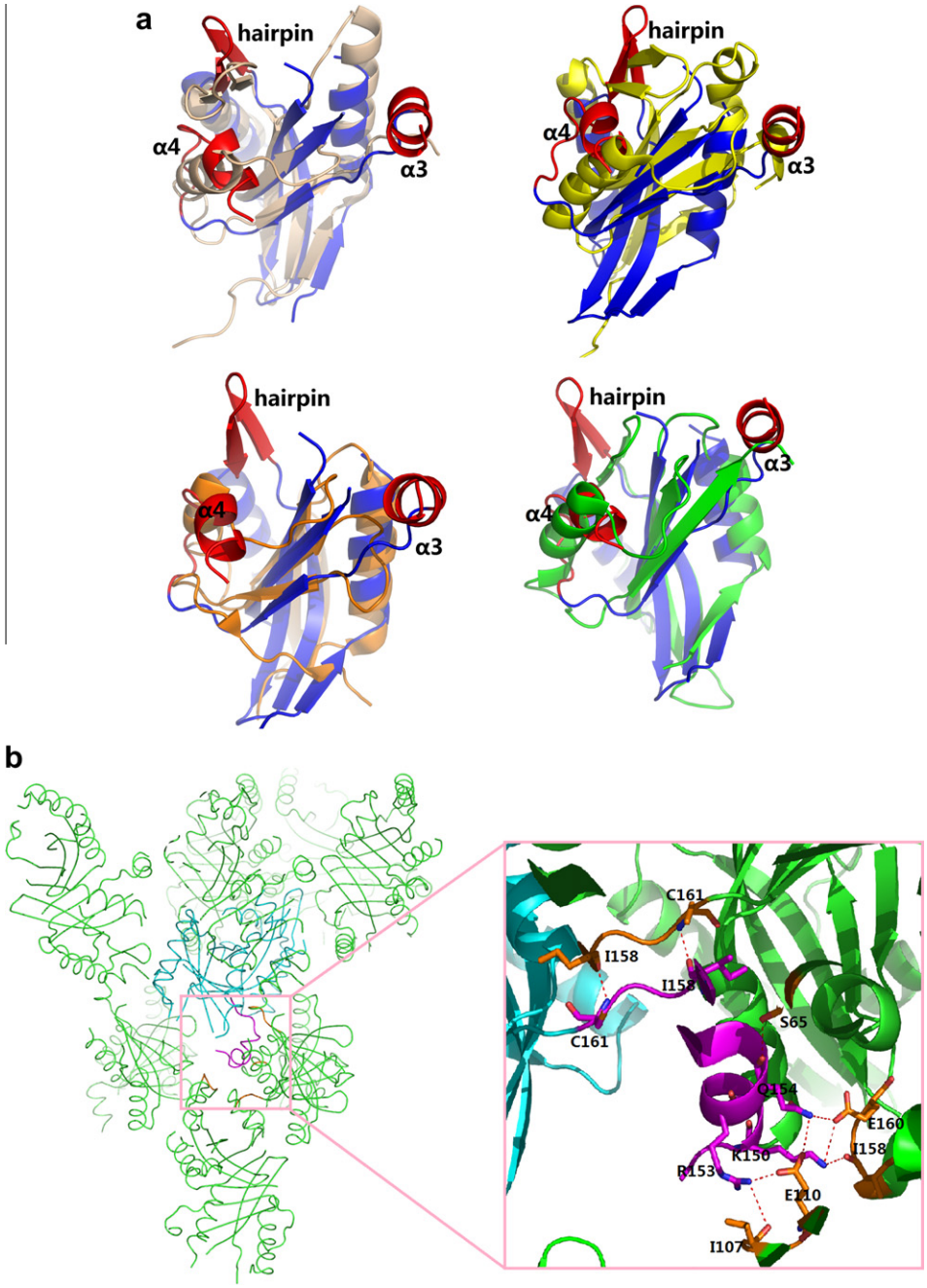

Fig. 5. (a) CSN6$^{51-187}$ (blue) is superimposed to MPN domains of Rpn8 (left above) (wheat), AMSH-LP (right above) (yellow), Af2198 (left below) (orange) and Prp8 (right below) (green). The regions of CSN6 are different from others in red colour. (b) Crystal packing of the CSN6 MPN domain. Helix α3 and the following loop (magenta) in the central (cyan) molecule make interactions with several regions (orange) of neighbouring molecules (green). The hydrogen and salt bonds involved in interactions are shown in the inset, and these residues are labelled.

tions demonstrate that α4 may participate in ubiquitin or ubiquitin-like proteins binding.

Another unique feature is found in the β-hairpin, which represents an open conformation in our structure, rather than locks toward the metal binding pocket in other JAMM family members [15–19]. This hairpin has been proposed to interact with ubiquitin in the deubiquitination process [18]. In principle, the hairpin must undergo structural variation to allow the substrate access to the active site. However, none of MPN structures exhibits a considerable plasticity for this hairpin except CSN6$^{51-187}$. In the case of AMSH-LP, Asp321 in the intervening loop closes down onto the active site, and it is well ordered regardless of whether the substrate is free or not [18,19]. Likewise, Asp65 in Rpn8 and Ser2235 in Prp8 block their putative active sites [15–17]. Unlike the structures mentioned above, the corresponding residue Asp109 in CSN6$^{51-187}$ is flexible with high temperature factors (Fig. 4B). Thus, this hairpin in CSN6$^{51-187}$ represents a flexible open state, perhaps to ensure correct localization of substrate during CSN5 catalyzed deneddylation process.

At last, other classic domains could not be expressed as soluble proteins without extension, except the Af2198 [16,18–19]. At the same time, CSN5 expression results support observations (unpublished data) mentioned above. In contrast, the MPN domain in CSN6 is soluble during expression. The aliphatic and instability indices (95.33 and 37.17, respectively) also indicate that CSN6$^{51-187}$ is a stable protein. It is, therefore, reasonable

to believe that the MPN domain of CSN6 is an independent structure and function, not a subdomain like other MPN-containing proteins.

In conclusion, CSN6 MPN domain is an interaction domain instead of a metalloprotease, and it may represent a new function based on structural comparisons.

4. PDB accession number

Atomic coordinates and structure factors of CSN651–187 were deposited in the Protein Data Bank under accession number 4E0Q.

Acknowledgements

We thank the staff at SSRF beamline. We also thank Dr Haifeng Hou and Kun Qu for helpful discussion.

This work was supported by the grants from the National Basic Research Program of China (2009CB918600), the National Natural Science Foundation of China (10979005).

Appendix A. Supplementary data

Supplementary data associated with this article can be found, in the online version, at http://dx.doi.org/10.1016/j.febslet.2012.03.029.

References

[1] Wei, N. and Deng, X.W. (2003) The COP9 signalosome. Annu. Rev. Cell Dev. Biol. 19, 261–286.
[2] Sharon, M., Mao, H., Erba, E.B., Stephens, E., Zheng, N. and Robinson, C.V. (2009) Symmetrical modularity of the COP9 signalosome complex suggests its multifunctionality. Structure 17, 31–40.
[3] Krissinel, E. and Henrick, K. (2007) Inference of macromolecular assemblies from crystalline state. J. Mol. Biol. 372, 774–797.
[4] Aravind, L. and Ponting, C.P. (1998) Homologues of 26S proteasome subunits are regulators of transcription and translation. Protein Sci. 7, 1250–1254.
[5] Hofmann, K. and Bucher, P. (1998) The PCI domain: a common theme in three multiprotein complexes. Trends Biochem. Sci. 23, 204–205.
[6] Hoareau, A.K., Bochard, V., Rety, S. and Jalinot, P. (2002) Association of the mammalian proto-oncoprotein Int-6 with the three protein complexes eIF3, COP9 signalosome and 26S proteasome. FEBS Lett. 527, 15–21.
[7] Wei, N., Chamovitz, D.A. and Deng, X.W. (1994) Arabidopsis COP9 is a component of a novel signaling complex mediating light control of development. Cell 178, 117–124.
[8] Lee, M.H., Zhao, R.Y., Phan, L. and Yeung, S.-C.J. (2011) Roles of COP9 signaolsome in cancer. Cell Cycle 10, 3057–3066.
[9] Lyapina, S., Cope, G., Shevchenko, A., Serino, G., Tsuge, T., Zhou, C., Wolf, D.A., Wei, N. and Deshaies, R.J. (2001) Promotion of NEDD-CUL1 conjugate cleavage by COP9 signalosome. Science 292, 1382–1385.
[10] Cope, G.A., Suh, G.S., Aravind, L., Schwarz, S.E., Zipursky, S.L., Koonin, E.V. and Deshaies, R.J. (2002) Role of predicted metalloprotease motif of Jab1/ Csn5 in cleavage of NEDD8 from CUL1. Science 298, 608–611.
[11] Zhao, R.Y. et al. (2011) Subunit 6 of the COP9 signalosome promotes tumorigenesis in mice through stabilization of MDM2 and is upregulated in human cancers. J. Clin. Invest. 121, 851–865.
[12] Holm, L., Kaariainen, S., Rosenstrom, P. and Schenkel, A. (2008) Searching protein structure databases with DaliLite v. 3. Bioinformatics 24, 2780–2781.
[13] Tran, H.J., Allen, M.D., Lowe, J. and Bycroft, M. (2003) Structure of the Jab1/MPN domain and its implications for proteasome function. Biochemistry 42, 11460–11465.
[14] Ambroggio, X.I., Rees, D.C. and Deshaies, R.J. (2004) JAMM: a metalloprotease-like zinc site in the proteasome and signalosome. PLoS Biol. 2, 114–119.
[15] Sanches, M., Alves, B.S., Zanchin, N.I. and Guimaraes, B.G. (2007) The crystal structure of the human Mov34 MPN domain reveals a metal-free dimer. J. Mol. Biol. 370, 846–855.
[16] Zhang, L. et al. (2007) Crystal structure of the C-terminal domain of splicing factor Prp8 carrying *Retinitis pigmentosa* mutants. Protein Sci. 16, 1024–1031.
[17] Pena, V., Liu, S., Bujnicki, J.M., Luhrmann, R. and Wahl, M.C. (2007) Structure of a multipartite protein– protein interaction domain in splicing factor Prp8 and its link to *Retinitis pigmentosa*. Mol. Cell 25, 615–624.
[18] Sato, Y. et al. (2008) Structural basis for specific cleavage of Lys 63-linked polyubiquitin chains. Nature 455, 358–362.
[19] Daies, C.W., Paul, L.N., Kim II, M. and Das, C. (2011) Structural and thermodynamic comparison of the catalytic domain of AMSH and AMSH-LP: nearly identical fold but different stability. J. Mol. Biol. 413, 416–439.
[20] Fernandez-Escamilla, A.M., Rousseau, F., Schymkowitz, J. and Serrano, L. (2004) Prediction of sequence-dependent and mutational effects on the aggregation of peptides and proteins. Nature Biotechnol. 22, 1302–1306.
[21] Delano, W.L. (2002) PyMOL Molecular Viewer. <http://www.pymol.org/>.
[22] Thompson, J.D., Higgins, D.J. and Gibson, T.J. (1994) CLUSTAL W: improving the sensitivity of progressive multiple sequence alignment through sequence weighting, position-specific gap penalties and weight matrix choice. Nucleic Acid Res. 22, 4673–4680.
[23] Gouet, P., Courcelle, E., Stuart, D.I. and Metoz, F. (1999) ESPript: multiple sequence alignments in PostScript. Bioinformatics 15, 305–308.
[24] Landau, M., Mayrose, I., Rosenberg, Y., Glaser, F., Martz, E., Pupko, T. and Ben-Tal, N. (2005) ConSurf 2005: the projection of evolutionary conservation scores of residues on protein structures. Nucleic Acids Res. 33, W299–302.
[25] Svergun, D.I., Petoukhov, M.V.M. and Koch, H.J. (2001) Determination of domain structure of proteins from X-ray solution scattering. Biophys. J. 76, 2879–2886.
[26] Svergun, D.I. (1999) Restoring low resolution structure of biological macromolecules from solution scattering using simulated annealing. Biophys. J. 76, 2879–2886.
[27] Bellare, P., Kutach, A.K., Rines, A.K., Guthrie, C. and Sontheimer, E.J. (2006) Ubiquitin binding by a variant Jab1/MPN domain in the essential pre-mRNA splicing factor Prp8p. RNA 12, 292–302.
[28] Rosel, D. and Kimmel, A.R. (2006) The COP9 signalosome regulates cell proliferation of *Dictyostelium discoideu*. Eur. J. Cell Bio. 85, 1023–1034.
[29] Chamovitz, D.A. (2009) Revisiting the COP9 signalosome as a transcriptional regulator. EMBO Rep. 10, 352–358.
[30] Schweichheimer, K. and Isono, E. (2010) The COP9 signalsome and its role in plant development. Eur. J. Cell Bio. 89, 157–162.
[31] Serino, G. and Deng, X.W. (2003) The COP9 signalosome: Regulating plant development through the control of proteolysis. Annu. Rev. Plant Biol. 54, 165–182.